Extended Abstracts of the 2013 International Conference on Solid State Devices and Materials, Fukuoka, 2013, pp1182-1183

Diffusion Coefficients of Impurity Atoms in $BaSi_2$ Epitaxial Films Grown by Molecular Beam Epitaxy

N. Zhang[1], K. Nakamura[1], M. Baba[1], K. Toko[1], and T. Suemasu[1, 2]

[1] Institute of Applied Physics, University of Tsukuba, Tsukuba, Ibaraki 305-8573, Japan
Phone: +81-29-853-5472 E-mail: bk200913016@s.bk.tsukuba.ac.jp
[2] CREST-JST, Chiyoda, Tokyo 102-0075, Japan

Abstract

Sb layers deposited on $BaSi_2$ epitaxial films on Si(111) substrates were annealed at different temperatures, and the diffusion coefficients of Sb were evaluated using secondary ion mass spectrometry with Cs^+ ions. The activation energies of lattice and grain boundary diffusions in $BaSi_2$ are 0.64 eV and 1.20 eV, respectively.

1. Introduction

$BaSi_2$ has the bandgap of about 1.3 eV and a large optical absorption coefficient, reaching 3×10^4 cm^{-1} at 1.5 eV experimentally [1-3]. In addition, the minority-carrier diffusion length in undoped $BaSi_2$ films reaches a value as large as 10 μm [4]. Also *a*-axis-oriented $BaSi_2$ can be grown epitaxially on Si(111) and Si(001) surfaces [5-7]. Therefore, $BaSi_2$ is considered one of the new materials for high-efficiency thin-film solar cells. There is a requirement to control the conductivity of $BaSi_2$ by impurity doping to make a *p-n* junction which is the basic structure of a solar cell. Impurities with small diffusion coefficients and large carrier concentrations are needed. Up to the present, we have already done a lot of studies on Al and B which are *p*-type dopants for $BaSi_2$ [8,9]. However there have been no reports about diffusion coefficients of *n*-type dopants for $BaSi_2$. In this study, we aimed to evaluate the lattice and grain boundary (GB) diffusion coefficients of Sb, the *n*-type dopant for $BaSi_2$.

2. Experimental procedure

A two-stage growth method was applied, that is, reactive deposition epitaxy (RDE; Ba deposition on hot Si) for $BaSi_2$ template layers, and the subsequent molecular beam epitaxy (MBE; codeposition of Ba and Si on Si) at 580 ºC to form a 600-nm-thick *a*-axis-oriented $BaSi_2$ epitaxial film on Si(111). Then, an approximately 100-nm-thick Sb film was evaporated onto the undoped $BaSi_2$ layers at room temperature (RT) by vacuum evaporation. Then the sample was cut into several pieces and annealed in an Ar atmosphere at different temperatures and durations, that is, 200 ºC for 4 h, 250 °C for 4 h, and 300 ºC for 1 h. Finally we investigated the depth profiles of Sb in $BaSi_2$ using secondary ion mass spectrometry (SIMS) measurement with Cs^+ ions, and evaluated its lattice and GB diffusion coefficients. Crystalline quality of grown films was characterized by reflection high-energy electron diffraction (RHEED), θ-2θ X-ray diffraction (XRD), and plan-view transmission electron microscopy (TEM) along the $BaSi_2$[100] azimuth.

3. Results and Discussion

A streaky RHEED pattern and (100)-oriented diffractions in the XRD pattern in Fig. 1 show that *a*-axis-oriented epitaxial layers were formed.

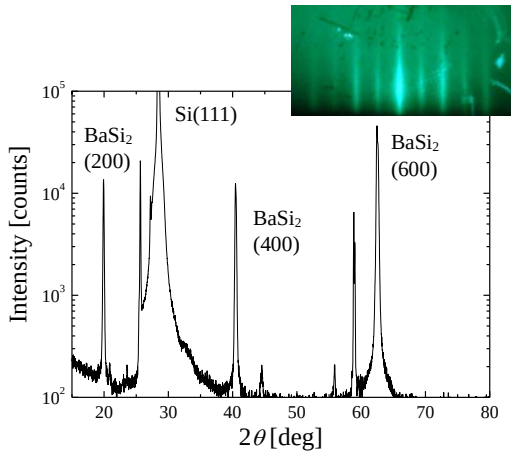

Fig. 1 RHEED pattern observed along Si [11-2] and *θ-2θ* XRD pattern of undoped $BaSi_2$

Figure 2 shows the bright-field plan-view TEM image of the undoped $BaSi_2$ film observed along $BaSi_2$ [100]. Because of the three epitaxial variants rotated by 120º around the surface normal of Si(111), grain boundaries exist in the epitaxial layers. Thus, not only the lattice diffusions, but also GB diffusions must be considered.

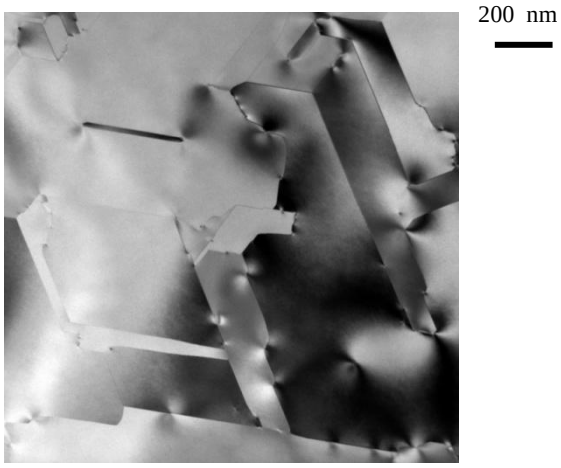

Fig. 2 Bright-field plan-view TEM image observed along $BaSi_2$[100].

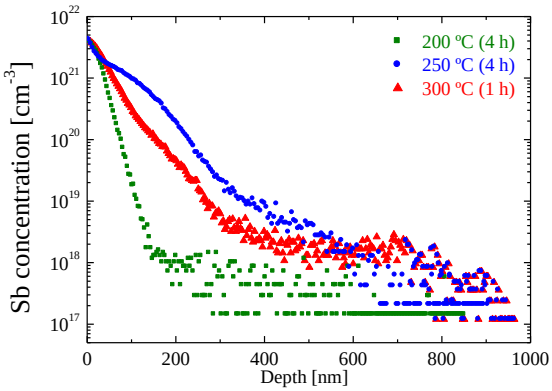

Fig. 3 SIMS depth profiles of Sb atoms after annealing at 200 °C for 4 h, 250 °C for 4 h, and 300 °C for 1 h.

Figure 3 shows the depth profiles of Sb atoms in $BaSi_2$ layers after annealing at 200 ºC for 4 h, 250 °C for 4 h, and 300 ºC for 1 h. To fit these experimentally obtained SIMS profiles, Eqs. (1) and (2) were adopted for lattice diffusion and GB diffusion, respectively. The concentration distribution $C(x, t)$ of impurity atoms due to the lattice diffusion is given by Eq. (1) [10], where x=0 is set at the Sb/$BaSi_2$ interface, and C_0 the Sb concentration at x=0, D_l the lattice diffusion coefficient, and t the annealing duration.

$$C(x,t) = C_0 \mathrm{erfc}(x/2\sqrt{D_l t}) \quad (1)$$

$$s\delta D_{GB} = 1.332(D_l/t)^{1/2}\left(-\partial \ln C(x,t)/\partial x^{6/5}\right)^{-5/3} \quad (2)$$

Meanwhile, the concentration distribution due to GB diffusion follows Eq. (2) [11], where s is the segregation factor, δ the grain boundary width, and D_{GB} the GB diffusion coefficient.

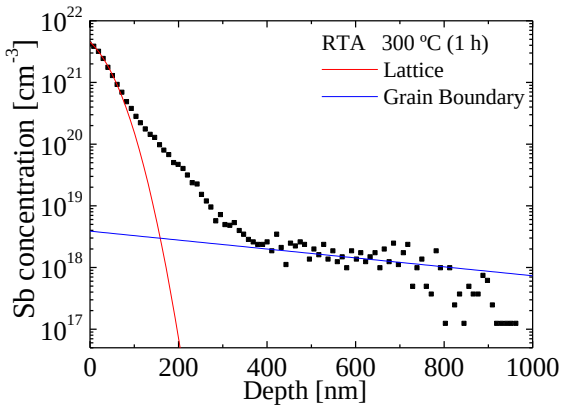

Fig.4 Measured and simulated SIMS profiles of Sb in the undoped $BaSi_2$ film after annealing at 300 ºC for 1 h

Figure 4 gives an example for the measured and simulated SIMS profiles of Sb in the undoped $BaSi_2$ film, annealed at 300 ºC for 1 h. We also fitted the other two profiles in the same way. Figure 5 shows the Arrhenius plots for the obtained lattice diffusion coefficient D_l and sD_{GB}, the product of segregation factor and GB diffusion coefficient of Sb atoms. Diffusion coefficients of impurity atoms in other silicides are also shown for comparison. Here, we set the GB width δ to be 0.5 nm [11]. We see that the diffusion coefficients of Sb are found to be much larger than those of B, and almost the same as those of Al in $BaSi_2$ [8, 12]. The activation energies of lattice diffusion and GB diffusion for Sb in $BaSi_2$ are 0.64 eV and 1.20 eV, respectively. On the basis of these results, we conclude that Sb atoms easily diffuse in $BaSi_2$. As a next step, we plan to go into As, another n-type dopant candidate.

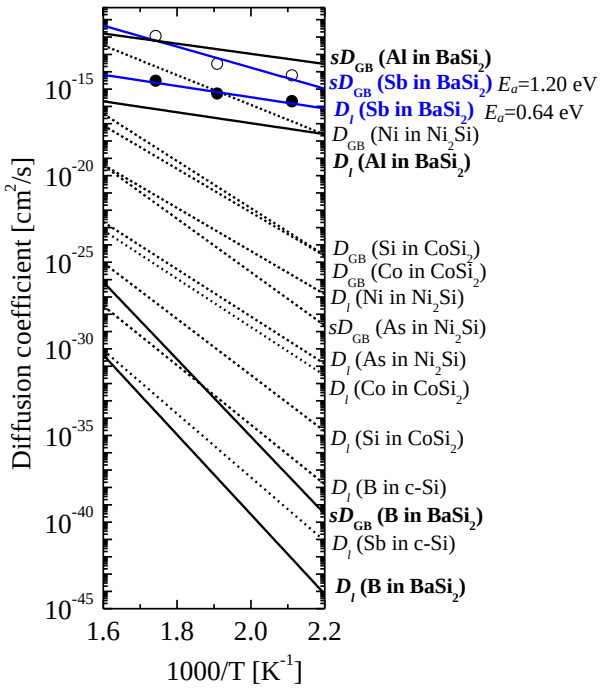

Fig. 5 Arrhenius plots for the lattice diffusion coefficient D_l and the product of segregation factor and GB diffusion coefficient sD_{GB} of Sb and other atoms.

4. Conclusions

The lattice and GB diffusion coefficients of Sb were evaluated using the $BaSi_2$ epitaxial films capped with Sb layers. The activation energies of diffusion of Sb in the undoped $BaSi_2$ are 0.64 eV and 1.20 eV for lattice diffusion and GB diffusion, respectively.

[1] K. Morita *et al.*, Thin Solid Films 508 (2006) 363.
[2] D. B. Migas *et al.*, Phys. Status Solidi B 244 (2007) 2611.
[3] K. Toh *et al.*, Jpn. J. Appl. Phys. 50 (2011) 068001.
[4] M. Baba et al., J. Cryst. Growth 348 (2012) 75.
[5] R. A. Mckee *et al.*, Appl. Phys. Lett. 59 (1991) 782.
[6] Y. Inomata *et al.*, Jpn. J. Appl. Phys. 43 (2004) L478.
[7] K. Toh *et al.*, J. Cryst. Growth 345 (2012) 16.
[8] K. Nakamura *et al.*, J. Cryst. Growth, doi.org/10.1016/j.jcrysgro.2012.12.051
[9] M. Ajmal Khan *et al.*, Appl. Phys. Lett. 102 (2013) 112107.
[10] S.M.Sze, Physics of Semiconductor Devices, John Wiley &Sons (2007).
[11] B.S. Bokstein *et al.*, Phys. Metals Metallogr. 6 (1958) 81.
[12] K. Nakamura *et al.*, J. Appl. Phys. 113 (2013) 05311.